Long-Ranged Orientational Order in Dipolar Fluids

B. Groh and S. Dietrich

Fachbereich Physik, Bergische Universität Wuppertal, D-42097 Wuppertal, Federal Republic of Germany

(Received 22 November 1993)

Based on density-functional theory we study the occurrence of a ferroelectric phase in Stockmayer fluids. Because of the long-ranged dipolar forces the corresponding bulk phase diagrams depend on both the shape of the sample and the character of the dielectric surrounding. For ellipsoidal samples with different aspect ratios at high temperatures we find a line of critical points, whereas at temperatures below a tricritical point the phase transition is first order. The behavior near the continuous phase transitions is analyzed by a systematic Landau expansion.

PACS numbers: 64.70.−p, 61.25.Em, 64.60.Kw, 77.80.−e

Ferromagnetism is a paradigm for spontaneous long-ranged orientational order within a lattice structure. Since for most materials the Curie temperature is less than the melting temperature of the lattice, one could be inclined to suppose that long-ranged *positional* order is a prerequisite for long-ranged *orientational* order. However, various counterexamples show that under certain circumstances even the liquid state of condensed matter can sustain long-ranged orientational order. It has been shown recently that ferromagnetism based on short-ranged forces can persist in the liquid phase of two-dimensional [1] and three-dimensional [2] fluids with internal quantum states. The best known example of purely orientationally ordered liquids is the nematic phase of liquid crystals. In 1916 Born [3] conjectured that in this case the orientational order is induced by dipolar interactions. Since then, however, it became clear that the short-ranged steric forces of sufficiently elongated hard particles [4] as well as long-ranged quadrupolar-like interactions [5] can lead to the formation of the nematic phase. Only recently molecular dynamics simulations by Wei and Patey [6] and Weis *et al.* [7] provided evidence that an orientationally ordered liquid can form in dipolar hard or soft sphere fluids, for which the dipolar interaction represents the *only* orientational dependent force. This finding is supported by the occurrence of orientational instabilities in integral equation theories of these fluids [8,9]. Both from a fundamental point of view and for technical applications it is interesting that these phases are not only nematic but also ferroelectric. A physical system to which these models also probably apply is a ferrofluid, i.e., a suspension of small (50–100 Å) particles carrying permanent magnetic dipole moments [10].

In this contribution we present an analytic theory for the thermodynamic properties of Stockmayer fluids, which consist of spherical particles interacting via a Lennard-Jones potential $w_{LJ}(r)=4\epsilon[(\sigma/r)^{12}-(\sigma/r)^{6}]$ plus dipolar forces between the permanent dipole moments of the particles:

$$w_{dip}(\mathbf{r},\omega,\omega')=-\frac{m^2}{r^3}\{3[\hat{\mathbf{m}}(\omega)\hat{\mathbf{r}}][\hat{\mathbf{m}}(\omega')\hat{\mathbf{r}}] - \hat{\mathbf{m}}(\omega)\hat{\mathbf{m}}(\omega')\}\Theta(r-\sigma) \quad (1)$$

Here $\mathbf{m}$ is the dipole moment, $\hat{\mathbf{m}}$ and $\hat{\mathbf{r}}$ are unit vectors, and Θ is the Heaviside function. This somewhat more realistic model takes into account also the long-ranged dispersion forces; in contrast to the dipolar hard or soft sphere fluids [11] it exhibits the common liquid-gas phase transition [12]. By using an appropriate density-functional theory [13], whose thorough analysis overcomes difficulties encountered in previous approaches [14], we map out the fluid parts of the phase diagram finding indeed a ferroelectric phase. It turns out that the bulk phase diagram depends on both the shape of the sample and the dielectric constant of its surrounding. An elongated sample is considerably more favorable for the formation of the ferroelectric phase than a spherically shaped sample which has been implicitly assumed in the molecular-dynamics simulations of Refs. [6,7] by using the Ewald summation technique [15]. The ferroelectric and the isotropic phases are separated by a line of critical points which turns into a first-order transition at a tricritical point. The critical exponents and the corresponding amplitudes near the continuous phase transitions are determined analytically within mean-field theory by means of a systematic Landau theory. These results pinpoint the importance of the correct performance of the thermodynamic limit as well as the relevance of boundary conditions for the bulk behavior of such fluids and they provide a guideline for future numerical simulations which can hardly sweep the full parameter space of these systems.

A ferroelectric nematic fluid is described by the mean number density ρ and the distribution $a(\omega)$ of the molecular orientation $\omega=(\theta,\phi)$ with $\int d\omega\, a(\omega)=1$. According to Barker and Henderson [16] the interaction potential $w=w_{LJ}+w_{dip}$ is divided into a short-ranged repulsive reference part $w_{ref}(r)=\Theta(\sigma-r)w(\mathbf{r},\omega,\omega')$ and a long-ranged attractive excess part $w_{ex}(\mathbf{r},\omega,\omega')=\Theta(r-\sigma)$

0031-9007/94/72(15)/2422(4)$06.00

$\times w(\mathbf{r},\omega,\omega')$ which is treated as a perturbation [17]. Our analysis is based on the following grand-canonical variational functional [13] for a sample with a single domain:

$$\frac{1}{V}\Omega[\rho,\{a(\omega)\},T,\mu]=f_{\rm ref}^{\rm HS}(\rho,T)+\frac{\rho}{\beta}\int d\omega\, a(\omega)\ln[4\pi a(\omega)]+\frac{1}{V}\Omega_{\rm int}-\mu\rho\,, \tag{2}$$

where V, T, and μ denote the volume of the fluid, its temperature, and chemical potential. For the free energy density of the hard sphere reference fluid, which is given by the first term in Eq. (2), we use the expression of Carnahan and Starling [18] and employ a temperature dependent hard sphere diameter [19] which takes into account the soft repulsive part of the interaction potential. The second contribution to the grand-canonical potential stems from the additional entropy due to the orientational degrees of freedom. It vanishes for an isotropic fluid for which $a(\omega)=1/(4\pi)$. The interaction contribution,

$$\Omega_{\rm int}=\frac{\rho^2}{2\beta}\int_V d^3r\int_V d^3r'\int d\omega\, d\omega'\, a(\omega)a(\omega')e^{-\beta w_{\rm ref}(\mathbf{r}-\mathbf{r}')}(1-e^{-\beta w_{\rm ex}(\mathbf{r}-\mathbf{r}',\omega,\omega')})\,, \tag{3}$$

follows from using the low-density approximation $g^{(2)}\approx\exp(-\beta w)$ for the pair distribution function [13]. The orientational distribution depends only on the angle θ and can be expressed in terms of Legendre polynomials:

$$2\pi a(\omega)=\bar{a}(\cos\theta)=\sum_{l=0}^{\infty}a_l P_l(\cos\theta)\,. \tag{4}$$

We consider a finite volume which has the shape of a rotational ellipsoid with two short axes of length R and one long axis of length kR. The polarization points along the long axis [20]. By performing the limit $R\to\infty$ for fixed k and carefully taking into account the long-ranged nature of the dipolar interaction, after a lengthy calculation we find that the grand-canonical potential is indeed an extensive quantity proportional to the volume of the sample in the thermodynamic limit and takes on the following *shape dependent* form:

$$\lim_{V\to\infty}\frac{1}{V}\Omega_{\rm int}=\rho^2\sum_{l=0}^{\infty}u_l a_l^2\,, \tag{5}$$

where the coefficients u_l are given by

$$u_l=-\frac{1}{\beta}\frac{4\sqrt{\pi}(-1)^l}{(2l+1)^{3/2}}\int_\sigma^\infty dr_{12}r_{12}^2\int d\omega\, d\omega'\tilde{f}(r_{12},\omega,\omega',\omega_{12})\Phi_{l10}^*(\omega,\omega',\omega_{12})-\frac{8\pi}{9}I(k)m^2\delta_{l,1}\,. \tag{6}$$

Here $\tilde{f}=\exp(-\beta\omega_{\rm ex})-1$ is the Mayer function and the functions $\Phi_{l_1l_2l}$ form a complete set of functions that are invariant under simultaneous rotation of the three solid angles ω, ω', and ω_{12} [13,21]. The function $I(k)$ describing the shape dependence of the grand-canonical potential, which enters only via the coefficient u_1, is given by

$$I(k)=\frac{k^2+2}{3(k^2-1)}-\frac{k}{(k^2-1)^{3/2}}\ln(k+\sqrt{k^2-1})\,. \tag{7}$$

A macroscopic calculation of the electrostatic energy of a homogeneously polarized ellipsoid gives $W_{\rm el}/V=2\pi D(k)P^2$ with the depolarization factor $D(k)=\frac{1}{3}-I(k)$ [22] which yields the same shape dependence of the free energy density as our microscopic theory. If the polarized fluid is surrounded by a dielectric container characterized by the dielectric constant ϵ, the induced polarization in this surrounding medium generates an additional reaction field which leads to a corresponding contribution to the free energy density. With the definition

$$I(k)-D(k)\frac{(\epsilon-1)[D(k)-1]}{\epsilon-D(k)(\epsilon-1)}=I(k_{\rm eff}(k,\epsilon)) \tag{8}$$

for any k a system with $\epsilon\neq1$ can be mapped onto a system with $\epsilon=1$ and the aspect ratio $k_{\rm eff}(k,\epsilon)\geq k$ which has the same free energy density. For this reason in the following we confine ourselves to the case $\epsilon=1$.

The interaction contribution to the grand-canonical functional can be rewritten as

$$\lim_{V\to\infty}\frac{1}{V}\Omega_{\rm int}=\frac{\rho^2}{2}\int_{-1}^{1}dx\int_{-1}^{1}dx'\,\bar{a}(x)\bar{a}(x')K(x,x') \tag{9}$$

with the kernel

$$K(x,x')=\sum_{l=0}^{\infty}\frac{(2l+1)^2}{2}u_l P_l(x)P_l(x')\,. \tag{10}$$

Minimization of the grand-canonical functional with respect to the angular distribution $\bar{a}(x)$ leads to the integral equation

$$\bar{a}(x)=\frac{\exp[-\rho\beta\int_{-1}^{1}dx'\,\bar{a}(x')K(x,x')]}{\int_{-1}^{1}dx\exp[-\rho\beta\int_{-1}^{1}dx'\,\bar{a}(x')K(x,x')]}\,. \tag{11}$$

In order to compute the coefficients u_l we expand the Mayer function in Eq. (6) for small dipole moments m which allows us to perform the angular integrations analytically. We find $u_{l\geq2}\sim m^{2l}+O(m^{2l+4})$. By a lengthy algebraic manipulation using the orthogonality relation and sum rules for the functions $\Phi_{l_1l_2l}$ we have determined the expansion coefficients up to $O(m^8)$. Our numerical investigations show that this gives a satisfacto-

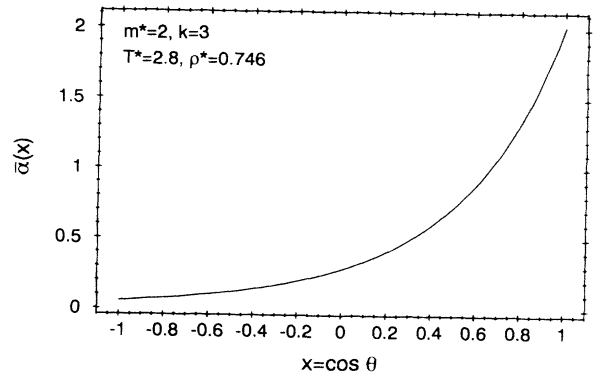

FIG. 1. A typical orientational distribution $\bar{\alpha}(\cos\theta)$ in the ferroelectric phase exhibiting a pronounced maximum at $\cos\theta=1$, i.e., in the direction of the long axis of the ellipsoidal sample.

ry accuracy for $m^*=(m^2/\epsilon\sigma^3)^{1/2}\leq 2$. Since we do not take into account the higher order terms, we can truncate the summation in Eq. (10) at $l=4$.

Because of the structure of $K(x,x')$ the solution of Eq. (11) has the form

$$\bar{\alpha}(x)=C\exp\left[-\rho\beta\sum_{l=0}^{4}(2l+1)u_l\alpha_l P_l(x)\right]. \tag{12}$$

A system of nonlinear equations for the variables C and $\alpha_1,\ldots,\alpha_4$ can be obtained from Eq. (11). Typical numerical solutions show that $\bar{\alpha}(x)$ exhibits a pronounced maximum at $x=1$, i.e., for orientations along the long axis of the ellipsoidal sample (see Fig. 1).

The phase diagram is determined by minimizing the grand-canonical potential with respect to the density ρ and $\bar{\alpha}(x)$. The fluid is described in terms of the reduced quantities m^*, $T^*=k_BT/\epsilon$, and $\rho^*=\rho\sigma^3$. Figure 2 displays the phase diagram for $m^*=2$ and $k=3$. At temperatures below the triple temperature T_3 an isotropic gas coexists with a ferroelectric liquid. Between T_3 and the critical temperature T_c coexistence of an isotropic gas and liquid or an isotropic and ferroelectric liquid is possible. At the tricritical point T_t the first-order transition between the isotropic and the ferroelectric fluid turns into a second-order transition. Near the tricritical point the density difference and the ferroelectric order parameter α_1 exhibit the mean-field critical exponents

$$\alpha_1\sim(T_t-T)^{1/2},\quad \rho_f-\rho_t\sim T_t-T,\quad T\nearrow T_t \tag{13}$$

along two phase coexistence for $T<T_t$ and

$$\alpha_1\sim(\mu-\mu_t)^{1/4},\quad \rho(T_t,\mu)-\rho_t\sim(\mu-\mu_t)^{1/2},\quad \mu\searrow\mu_t \tag{14}$$

for fixed $T=T_t$ where ρ_t and μ_t are the tricritical density and chemical potential. In three spatial dimensions these critical exponents are valid beyond mean-field theory [23]. On the other hand, upon approaching the phase boundary $\rho_{fc}(T)$ at a temperature $T_0>T_t$ one finds

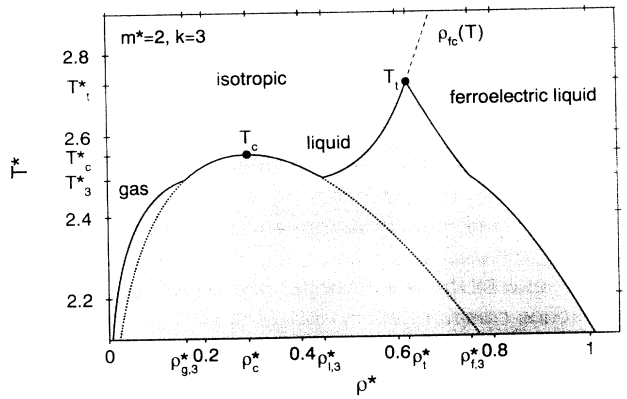

FIG. 2. Phase diagram for the dipole moment $m^*=2$ and the aspect ratio $k=3$. T_3, T_c, and T_t denote the triple, critical, and tricritical temperatures. Above the tricritical point there is a line of critical points $\rho_{fc}(T)$ given by the dashed curve. The dotted lines denote the two phase region of the isotropic gas and liquid if the ferroelectric phase is not taken into account. Within the shaded region there are no thermodynamically stable states.

$$\begin{aligned}&\alpha_1\sim(T_0-T)^{1/2},\quad T\nearrow T_0,\quad \mu \text{ fixed},\\ &\rho-\rho_{fc}(T_0)\sim T-T_0,\quad T\to T_0^{\pm},\quad \mu \text{ fixed},\end{aligned} \tag{15}$$

and

$$\begin{aligned}&\alpha_1\sim[\mu-\mu_{fc}(T_0)]^{1/2},\quad \mu\searrow\mu_{fc}(T_0),\quad T \text{ fixed},\\ &\rho-\rho_{fc}(T_0)\sim\mu-\mu_{fc}(T_0),\quad \mu\to\mu_{fc}(T_0)^{\pm},\quad T \text{ fixed}.\end{aligned} \tag{16}$$

If the critical fluctuations are taken into account, the exponent for α_1 in Eqs. (15) and (16) is expected to be replaced by $\beta\approx 0.35$. The mean-field exponents were derived from a systematic Landau expansion of the grand-canonical potential for small α_l, i.e., for small deviations from isotropy; this expansion also yields $\alpha_l=A_l(\rho/\rho_{fc}-1)^{l/2}$ for the higher order expansion coefficients of the orientational distribution with the amplitudes $A_1^2=\frac{5}{4}\times(3u_1-5u_2)/(u_1-5u_2)$ and $A_2=\frac{5}{2}u_1/(u_1-5u_2)$.

At larger aspect ratios the liquid-gas critical point vanishes, so that at all temperatures only two fluid phases exist (see Fig. 3; a similar topology of the phase diagram has been found in Refs. [1,2] which correspond to models with short-ranged interactions exhibiting no shape dependence). For small aspect ratios the formation of the ferroelectric phase affects the phase diagram only at high densities where a weakly first-order transition extends up to the highest densities considered. But in this case the formation of the ferroelectric fluid is probably preempted by freezing which is not captured by the present density-functional theory. Since the freezing transition is dominated by the short-ranged repulsive forces, it is expected to occur also for the Stockmayer fluid in the same density range as for hard spheres, i.e., at $\rho_f^*\simeq 0.95$ and $\rho_s^*\simeq 1.05$ [24]. (The close-packed structure corresponds to $\rho_s^*=\sqrt{2}$.)

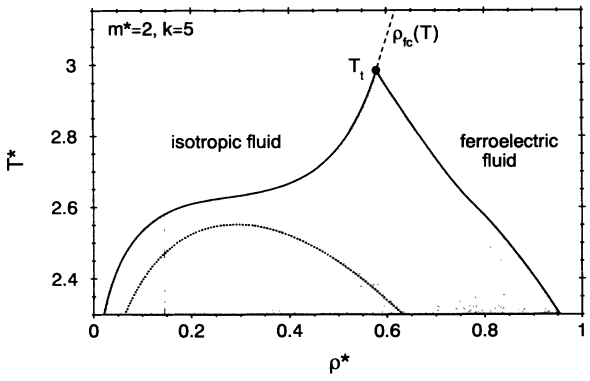

FIG. 3. Phase diagram for $m^*=2$, $k=5$, exhibiting only two phases, an isotropic fluid at low densities and a ferroelectric fluid at high densities. The dashed line $\rho_{fc}(T)$ indicates the line of second-order phase transitions above the tricritical temperature T_t. As in Fig. 2 the dotted curve is the phase diagram if the ferroelectric phase is not taken into account. Note that in comparison to Fig. 2 the critical point T_c has disappeared.

To summarize, our microscopic theory predicts the existence of a ferroelectric nematic phase in Stockmayer fluids. In this phase the free energy depends on the shape of the sample [Eq. (5)] as well as on the surrounding medium [Eq. (8)]. We have scanned the full phase diagrams for ellipsoidal samples of different aspect ratios which exhibit phase transitions of various characters. Obviously several further investigations lie ahead such as the study of domain formation and the use of more sophisticated density-functional theories, which are capable of describing the transition between the ferroelectric fluid and the solid phase.

[1] D. Marx, P. Nielaba, and K. Binder, Phys. Rev. Lett. **67**, 3124 (1991); S. Sengupta, D. Marx, and P. Nielaba, Europhys. Lett. **20**, 383 (1992).
[2] P. de Smedt, P. Nielaba, J. L. Lebowitz, J. Talbot, and L. Dooms, Phys. Rev. A **38**, 1381 (1988).
[3] M. Born, Sitz. Phys. Math. **25**, 614 (1916); Ann. Phys. (Leipzig) **55**, 221 (1918).
[4] L. Onsager, Proc. N.Y. Acad. Sci. **51**, 627 (1949).
[5] M. M. Telo da Gama, Mol. Phys. **52**, 585 (1984).
[6] D. Wei and G. N. Patey, Phys. Rev. Lett. **68**, 2043 (1992); Phys. Rev. A **46**, 7783 (1992).
[7] J. J. Weis, D. Levesque, and G. J. Zarragoicoechea, Phys. Rev. Lett. **69**, 913 (1992); J. J. Weis and D. Levesque, Phys. Rev. Lett. **71**, 2729 (1993).
[8] M. Kinoshita and M. Harada, Mol. Phys. **79**, 145 (1993).
[9] M. Kasch and F. Forstmann, J. Chem. Phys. **99**, 3037 (1993).
[10] R. E. Rosensweig, Sci. Am. **247**, No. 4, 124 (1982); *Ferrohydrodynamics* (Cambridge Univ. Press, Cambridge, 1985).
[11] J.-M. Caillol, J. Chem. Phys. **98**, 9835 (1993).
[12] M. E. van Leeuwen and B. Smit, Phys. Rev. Lett. **71**, 3991 (1993).
[13] P. Frodl and S. Dietrich, Phys. Rev. A **45**, 7330 (1992); Phys. Rev. E **48**, 3741 (1993).
[14] D. Wei, G. N. Patey, and A. Perera, Phys. Rev. E **47**, 506 (1993).
[15] S. W. de Leeuw, J. W. Perram, and E. R. Smith, Proc. R. Soc. London Ser. A **373**, 27 (1980); **388**, 177 (1983).
[16] J. A. Barker and D. Henderson, J. Chem. Phys. **47**, 4714 (1967).
[17] The analysis of the quantitative consequences of applying either alternative separation schemes for the repulsive part of the interaction potential [J. D. Weeks, D. Chandler, and H. C. Andersen, J. Chem. Phys. **54**, 5237 (1971); J. P. Hansen and I. R. MacDonald, *Theory of Simple Liquids* (Academic, London, 1986)] or of using the different approach of the so-called u expansion [G. Stell, J. C. Rasaiah, and H. Narang, Mol. Phys. **23**, 393 (1972); **27**, 1393 (1974)] is left to future studies.
[18] N. F. Carnahan and K. E. Starling, J. Chem. Phys. **51**, 635 (1969).
[19] J. A. Barker and D. Henderson, J. Chem. Phys. **47**, 2856 (1967).
[20] The consideration of the electrostatic energy shows that this orientation has the lowest free energy due to depolarization effects.
[21] C. G. Gray and K. E. Gubbins, *Theory of Molecular Fluids* (Clarendon, Oxford, 1984).
[22] R. Becker and F. Sauter, *Theorie der Elektrizität* (Teubner, Stuttgart, 1973), Vol. 1.
[23] I. D. Lawrie and S. Sarbach, in *Phase Transitions and Critical Phenomena*, edited by D. C. Domb and J. L. Lebowitz (Academic, London, 1984), Vol. 9, p. 1.
[24] W. G. Hoover and F. H. Ree, J. Chem. Phys. **49**, 3609 (1968).

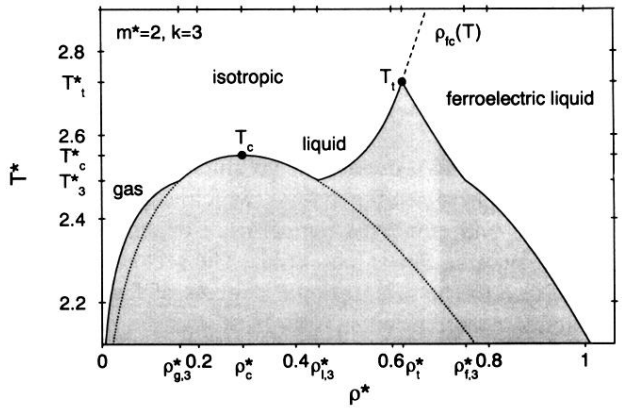

FIG. 2. Phase diagram for the dipole moment $m^* = 2$ and the aspect ratio $k = 3$. T_3, T_c, and T_t denote the triple, critical, and tricritical temperatures. Above the tricritical point there is a line of critical points $\rho_{fc}(T)$ given by the dashed curve. The dotted lines denote the two phase region of the isotropic gas and liquid if the ferroelectric phase is not taken into account. Within the shaded region there are no thermodynamically stable states.

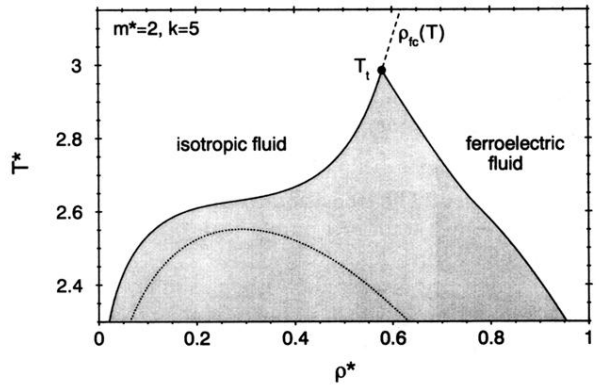

FIG. 3. Phase diagram for $m^* = 2$, $k = 5$, exhibiting only two phases, an isotropic fluid at low densities and a ferroelectric fluid at high densities. The dashed line $\rho_{fc}(T)$ indicates the line of second-order phase transitions above the tricritical temperature T_t. As in Fig. 2 the dotted curve is the phase diagram if the ferroelectric phase is not taken into account. Note that in comparison to Fig. 2 the critical point T_c has disappeared.